ELSEVIER

Carbohydrate Research 306 (1998) 479–491

CARBOHYDRATE RESEARCH

^{1}H NMR spectroscopy study of the dynamic properties of glycogen in solution by steady-state magnetisation measurement with off-resonance irradiation

Claire Wary [a]*, Hervé Desvaux [b], Marc Van Cauteren [c], Florent Vanstapel [d], Pierre G. Carlier [a], Philippe Jehenson [a]

[a] *Service Hospitalier Frédéric Joliot, C.E.A., F-91401 Orsay, France*

[b] *Service de Chimie Moléculaire, C.E.A./C.E. Saclay, F-91191 Gif-sur-Yvette, France*

[c] *Philips Medical Systems, Kohnan 2-13-37, Tokyo 108, Japan*

[d] *Biomedical NMR Unit, Department of Radiology, School of Medicine, Katholieke Universiteit Leuven, B-3000 Leuven, Belgium*

Received 25 June 1997; accepted 29 December 1997

Abstract

The dynamics of size-selected fractions of glycogen in solution have been investigated by proton NMR spectroscopy, using a recently described relaxation study method which relies on strong off-resonance irradiation. The dependence of the steady-state magnetisation on angle and intensity of the effective radio-frequency field was measured and compared to theoretical curves derived from different models of motion. Absence or presence of contributions to relaxation from molecular motions on the microsecond time scale can be tested with this method, without having to resort to models. We found that glycogen dipolar relaxation did not result from isotropic Brownian rotation, and despite some contribution from slow motion ($>1\,\mu$s) to relaxation in glycogen α-particles extracted from rat liver, bulk movement of the molecules did not appear to participate in averaging the dipolar term to zero. Whereas hepatic glycogen rat β-particles and commercial oyster glycogen displayed very similar relaxation properties, α-particles showed significantly different behaviour. However, all results were compatible with a diversity of movements within the molecule, ranging from freely rotating pyranoside rings through collective chain motion and possibly to bulk movement of the β sub-units within the α-particle.

Keywords: NMR; Glycogen; Macromolecular motion; Dipolar relaxation; Correlation times

1. Introduction

Glycogen, a storage form of D-glucose found throughout the animal kingdom and in certain plants, plays an essential role in glucose homeostasis.

* Corresponding author at present address: Unité de RMN, Institut de Myologie, Rue du Mur des Fermiers Généraux, Groupe Hospitalier Pitié-Salpêtrière, 47-83, boulevard de l'Hôpital, F-75651 Paris cedex 13, France; Tel: 33 (0) 1.42.16.58.96; Fax: 33 (0) 1.42.16.58.87; e-mail: cwary@myologie.infobiogen.fr

0008-6215/98/$19.00
PII S0008-6215(98)00005-6

Despite its very high molecular weight ($\geq 10^7$ Da), it is visible in both proton and carbon magnetic resonance [1,2]. Nevertheless, there have been reports of variation of lineshape and visibility of the resonances with molecular synthesis or degradation [3–5]. This is of particular concern for quantitative NMR spectroscopy studies of glycogen metabolism, including in vivo NMR spectroscopy of glycogen which is currently used in humans as a non-invasive tool in physiological, physiopathological and diagnostic metabolic studies [6–8]. It is therefore most important to acquire an in depth understanding of the structure and dynamics of the macromolecule which govern NMR relaxation mechanisms, but would also appear to be intricately linked to processes of glycogen synthesis and degradation (e.g., ref [9] and references therein). In this context, we report ^{1}H NMR spectroscopy measurements which allow characterisation of internal dynamics of glycogen on both the microsecond and nanosecond timescales.

The NMR visibility of the glycogen macromolecule itself remains something of an enigma. Indeed, for the roughly spherical β particles of randomly branched α-D glucopyranose ($\sim 10^7$ Da), the rotational correlation time can be estimated, according to the Debye equation [10], to be of the order of a microsecond. These β particles can aggregate to give larger α particles (up to over 10^9 Da), for which the correlation time would be of the order of hundreds of microseconds. If the NMR relaxation processes were governed by molecular motions on such time scales, the resonance of glycogen would be altogether too broad to be observed. This was already pointed out in the earliest work, where Sillerud and Shulman [2] found carbon longitudinal relaxation rates ($1/T_1$) which were too small to be compatible with the estimated Debye rotational correlation times of the molecule. However, since a single correlation time of about 4.6 ns accounted for the measured rates for all carbons of glycogen, they concluded that relaxation originated from movements of uniform substructures on this time scale. It has since been generally accepted that the visibility of glycogen must result from rapid internal motion and a number of experiments have aimed at understanding the underlying relaxation mechanisms. Zang et al. [11] measured temperature and magnetic field dependence of the carbon relaxation rates of glycogen, both in vitro and in vivo. Although the measured longitudinal relaxation rates were compatible with a single correlation time of 6.4 ns, supporting the hypothesis of important internal motion, they found it necessary to introduce a contribution from tumbling motions on a timescale of 10 μs, which was derived from the Debye equation, in order to account for the transverse relaxation rates, as well as a distribution of internal motions about 3.9 ns. In contrast, glycogen proton relaxation measured following recovery from selective and semi-selective inversions [12] lead to the conclusion that the rates measured at different B_0 fields were consistent with a single correlation time of 2.7 ns. The apparent discrepancy between these results may be due to the inherent drawback of the usual methods for studying relaxation. The amount of accessible experimental data is limited by the number of available B_0 fields, thus hindering a precise validation of the theoretical assumptions. A very different approach consisted in measuring carbon transverse relaxation times for samples in which size and structure were varied [13]. The authors observed multiexponential transverse relaxation for samples of natural abundance and [1-^{13}C] enriched glycogen, for α and β particles of different molecular weights, and for glycogen degraded to limit dextrin. They observed a distribution in T_2 values, which depended only minimally on molecular size and medium viscosity, together with a very narrow distribution of T_1 values in the same conditions. This was attributed to a distribution of dynamics within the molecule. A number of studies thus support the idea of a distribution of internal motions in glycogen, but the issue of whether or not overall reorientation of the molecule contributes to relaxation remains unclear, especially since no direct evidence of motion on the microsecond time scale has been reported.

In this paper, a method proposed by Goldman and Desvaux [14,15] was used to study the dynamic properties of glycogen in solution as a function of its size and origin. It relies on measurement of the steady-state magnetisation of the proton spins in the presence of a strong off-resonance radio-frequency (rf) irradiation, which characterises the proton relaxation. In distinction to the usual longitudinal and transverse relaxation time measurement methods, an unlimited number of points can be obtained at one B_0 field. This makes it possible to test directly the validity of the assumptions required to fit the data, and to investigate motions in the nanosecond range. Moreover, this method

enables the exploration of what we will refer to in the following as slow motions [16,17], i.e., motions of characteristic time scales larger than a few hundred nanoseconds. This time scale is typically of the order of the overall correlation time estimated for glycogen in a rigid sphere model. To explore this particular point, the method requires no assumption whatsoever regarding the motional model. Slow motions are essentially detected through variation of the steady-state magnetisation with the rf field amplitude B_1, whilst the tilt of the effective field remains constant [16]. The method has been applied to various samples of α and β glycogen particles for which the molecular weight dispersity was narrowed by selective gel-filtration, to study both slow motion contributions and dispersion of internal motions in the nanosecond time scale.

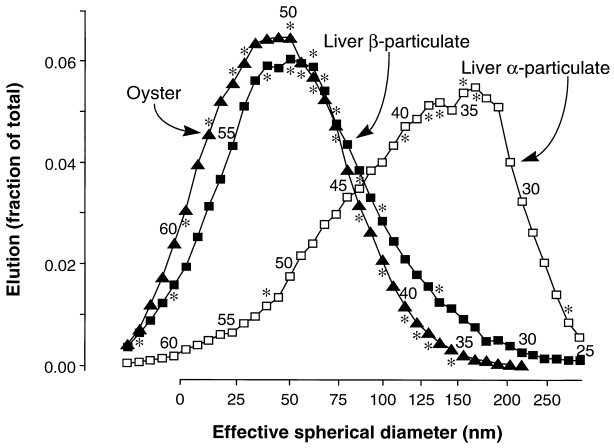

Fig. 1. Molecular weight distribution of α- (open symbols) and β-particulate (closed symbols) glycogen, of hepatic (square) and oyster (triangles) origin, determined by gel filtration on Sephacryl® Superfine S-1000. The abscissa (elution fraction indicated within the graph) is calibrated in effective spherical diameter (cf. Materials and methods). Fractions studied by NMR are marked with an asterisk (*).

2. Materials and methods

Preparation and characterisation of glycogen samples.—Three types of samples were used in this study. Glycogen was extracted from male Wistar derived Louvain *Pfd* rats, weighing about 250 g. Animals were starved and then refed to load their livers with glycogen [18]. α-Particulate glycogen *(a)* was obtained by non destructive aqueous phenol extraction [19]. Liver extraction with hot KOH (24%w:v) [20] yielded smaller β-particulate glycogen (*b*). Oyster (*oy*) glycogen (Type XI), extracted by a cold water procedure [21], was purchased from Sigma Chemicals (Kalamazoo, USA). Oyster glycogen has been shown to contain only low molecular weight particles [22].

To reduce molecular mass (MW) dispersity, glycogen samples (approximately 100 mg in 1 mL) were sized by gel filtration on a Sephacryl® Superfine S-1000 (Pharmacia, Uppsala, Sweden) column (34 cm, 10 mm diameter), developed (0.4 mL/min) with 150 mM NaCl, 0.1% (w:v) sodium dodecyl sulphate. The eluate was collected in fractions of 0.4 mL. The void volume (V_0:38% of bed volume) was determined by elution of polystyrene latex beads (500 nm; Monodisperse Polybead®, Polysciences, Warrington, USA). The gel exclusion volume (98% of bed volume) was determined from the elution behaviour of D-glucose. Published specifications were used to approximately calibrate the sampling axis (elution fraction or volume) in effective diameters [23]. Elution was monitored by measuring the absorbance of the glycogen–I_2 complex at a wave length of 460 nm [24]. The size distribution is shown in Fig. 1. The elution behaviour of α and β particles of glycogen reflected size distribution and not "unspecific" absorption to the gel matrix. Re-chromatography of a cut of heavy α-particulate glycogen resulted in no change in the elution pattern (not shown). The column elution profile confirmed published estimates [25–27] for the diameter of β (20–60 nm) and α (average 200 nm) particles of glycogen.

Samples were desalted by repeated EtOH (66%) precipitation, lyophilised and stored at −18 °C. Fractions selected for NMR study are marked with an asterisk in Fig. 1 ($n = 8$ for (*a*), $n = 8$ for (*b*) and $n = 14$ for (*oy*)), and are referred to by glycogen type and fraction number in the rest of the text. These were selected centrally to the distribution, except for one of lower MW and one of higher MW for all three glycogen types. In particular, low MW incomplete β particles might be expected to have a structure which differs from other samples in the distribution [28]. Prior to the NMR experiment, samples (2 to 5 mg) were dissolved in 300 μL of ^2H_2O (99.96% purity), with approximately 0.5% ultrapure grade sodium azide (Sigma Chemicals, Kalamazoo, USA) to prevent bacterial degradation of glycogen[1]. Samples were deoxygenated by

[1] Preliminary experiments showed that the azide did not modify glycogen H-1 relaxation, whereas even very limited degradation of the sample affected results.

flushing with argon. Comparison of control spectra acquired at the beginning and end of the experiments was used to validate stability of glycogen. No signs of free glucose and no changes in lineshape of the H-1(1→4) resonance of glycogen were observed.

NMR Acquisition.—All the proton spectra, except when otherwise specified, were collected at 300.13 MHz on a standard Bruker AMX system with a 5 mm reverse ^{1}H BB probe-head. The spectra collected at 500.13 MHz were obtained on Bruker AMX and DRX systems, with a 5 mm dedicated ^{1}H coil. Experiments were carried out at 37 °C. The free induction decays were acquired on 6 K complex data points, for a spectral width of 10 ppm, centred on the frequency of water.

The pulse sequence used to measure the steady-state magnetisation intensity aligned with the effective rf-field at an angle θ in the rotating frame, consists in an off-resonance rf irradiation followed by a 90° hard pulse applied on-resonance. The effective field is maintained at an angle θ (eq (1), Fig. 2)) and restored along the 0z axis by adiabatic rotation. The experiments involve measurement of the magnetisation of H-1(1→4) at different values of θ which may be obtained either by changing the radiofrequency amplitude ω_1, or by varying the offset frequency Δ. As long as slow motions do not contribute to the relaxation, the two methods are equivalent in theory. Experimentally, it is more convenient and more precise to modify Δ.

Measurement at different B_1 fields. When slow molecular motions are present and influence the relaxation rates, however, the steady-state magnetisation for a given angle θ will depend on the rf field amplitude ω_1 [16]. This property was used to detect evidence of contributions from slow movement to dipolar relaxation. The magnetisation was thus measured at six different values of the rf-field amplitude ω_1, ranging from 2.0 to 14.3 kHz, for up to 18 values of θ (between 2° and 60°). For the strongest B_1 fields, the smallest angles were not accessible since offsets Δ greater than 200 kHz were required for which the coil response was no longer adapted. At such strong ω_1 amplitudes, sample temperature could only be maintained stable (within 0.3 °C) by using a long repetition time (inter-scan delay was 30, 20, 16, 12, 8 and 8 s for 14.3, 12.2, 10.0, 7.5, 5.0 and 2.0 kHz, respectively), and reducing the duration of the irradiation to 0.9 s, the shortest possible time to reach steady-state. The experiments were carried out on glycogen fractions 26, 37, 38 and 40 of (*a*), 46, 47, 50 and 52 of (*b*) and 40, 47, 50, 59 and 63 of (*oy*).

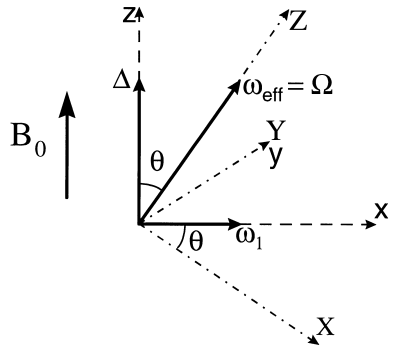

Fig. 2. The effective magnetic field created by strong rf-irradiation of amplitude $2\omega_1$ and at an offset Δ from the centre of the ^{1}H spectrum is aligned along 0Z in the rotating frame. It is tilted by an angle θ away from the external field B_0, along 0z in the laboratory frame.

Measurement of the magnetisation as a function of θ. Validity of theoretical assumptions used to derive expressions of the magnetisation as a function of θ, may only be accurately tested by precise measurement of decreasing steady-state magnetisation with increasing angle θ. Steady-state magnetisation intensities were therefore measured at 70 values of θ, by changing Δ. Two distinct values of ω_1 were nonetheless required, compromising between a large rf-field amplitude on the one hand (Ω must be large compared to the spread of chemical shifts) and avoiding too large offsets which introduce a dependence on probe response, on the other. Thirty-five angles from 1.0° to 20.0° were measured at $\omega_1 = 2.6$ kHz and 35 angles between 16.0° and 70.0° were measured at 5.4 kHz, at a B_0 field of 7.05 Tesla. The irradiation was applied during 1.3 s, the interscan delay was 6.3 s to allow full glycogen proton relaxation and the number of scans (multiples of 8) was increased as θ increased so as to compensate for decreasing signal intensity. For a better characterisation of the motional model, three samples (a35, b48, oy50) were re-examined at a B_0 field of 11.7 T ($\omega_1 = 2.6$ and 8.5 kHz for smaller and larger angles, respectively; adiabatic pulse duration of 1.3 s, interscan delay of 10 s, number of scans adjusted to maintain the signal to noise ratio).

Processing.—All data were initially processed using Bruker UXNMR software. Free induction decays were zero-filled to 8K complex points and filtered by exponential multiplication of 160 ms time constant, prior to Fourier transformation. After manually optimised phase correction and

automatic local baseline correction (2nd order polynomial, between 7 and 5 ppm) of the spectra, the area of the H-1(1→4) resonance of glycogen (linewidth at halfheight ~15 Hz) was integrated over 0.6 ppm. The integrated signal amplitudes of the experiments with 70 angles were plotted against θ, and fitted to various theoretical curves [2] running on a Sun Sparc20 workstation. The intensities of the experiments at different B_1 fields were plotted against θ, and fits for the six curves were obtained using the Excel 5.0 solver (Microsoft©, Newton algorithm) on a PC computer.

Theoretical background.—Principle of the method. The experiment consists in measuring the steady-state magnetisation of a system of n homonuclear spins 1/2 under strong off-resonance rf irradiation, at various values of the rf-field offset and amplitude. The general theory has been previously described [14,15]. In short, the steady-state magnetisation $\langle I_z^\alpha \rangle$ is aligned along the effective field axis 0Z and depends on the angle θ between the external field (0z axis) and the effective field in the frame rotating at the rf-field frequency ω:

$$\theta = \arctan \frac{\omega_1}{\Delta} \quad (1)$$

where $\Delta + \omega$ is the centre of the ^{1}H Larmor frequency spectrum, and $2\omega_1$ the off resonance rf-field amplitude. In this rotating frame, the effective field of amplitude Ω is:

$$\Omega = \sqrt{\omega_1^2 + \Delta^2} \quad (2)$$

The component of the magnetisation $\left(\langle I_z^\alpha \rangle\right)$ aligned with the effective field in the rotating frame is a solution of the following system of linear equations:

$$\sum_\beta \rho_{\alpha\beta}^\theta \langle I_z^\alpha \rangle + \sum_\beta \sigma_{\alpha\beta}^\theta \langle I_z^\beta \rangle = \sum_\beta \cos\theta \, (\rho_{\alpha\beta} + \sigma_{\alpha\beta}) I_0 \quad (3)$$

I_0 is the magnetisation at thermal equilibrium; $\rho_{\alpha\beta}^\theta$ and $\sigma_{\alpha\beta}^\theta$ are the self and cross dipolar relaxation rates along the effective field axis 0Z, due to the dipolar interaction between I^α and I^β; $\rho_{\alpha\beta}$, and $\sigma_{\alpha\beta}$ are the longitudinal self and cross dipolar relaxation rates as defined by Solomon [30].

[2] H. Desvaux, program available on request; Marquardt algorithm [29].

In the present experimental conditions (rf-field amplitude, molecular structure and size, and choice of angle θ), the relaxation rates $\rho_{\alpha\beta}^\theta$ and $\sigma_{\alpha\beta}^\theta$ may depend on the dipolar spectral density functions at frequencies 0, Ω, 2Ω, ω and 2ω [16]. Thus, by this method, motions of characteristic time scales could be explored both in the nanosecond range through the dependence on $J(\omega)$ and in the microsecond range (typically greater than 0.2 μs in the experiments described here) through $J(\Omega)$.

Models of motion. Further exploration of the characteristics of relaxation requires a solution to eq (3), which depends on a model for molecular motion. In the case of the glycogen molecule, we considered several models which seemed reasonable with respect to prior knowledge of structure and dynamics, which we will briefly summarise.

Under electron microscopy, β particles are present as oblate ellipsoids with axes ranging from 20 to 60 nm [25–27]. These particles (up to 100) may aggregate into larger α particles, which can reach a diameter of over 200 nm [25,26]. Global tumbling of α particles will impart isotropic rotational motions upon β sub-particles. Packing of β particles has not been analysed in detail [26]. Dense packing will result in a more viscous micro-environment, which may affect allowed rotational motions of the β sub-units. A wide distribution in molecular weight of β- and especially α-particulate glycogen (cf. Fig. 1) would result in a dispersion of long overall correlation times. Glycogen β particles consist largely of linear chains of 10 to 14 D-glucosyl moieties linked α-(1→4). These branch into new chains, by α-(1→6) D-glycosidic bonds, resulting in an irregularly branched structure [22]. Studies on related amylose [31] and oligosaccharides [32] suggest that internal (anisotropic) motions can be accommodated. The pyranoside ring itself, exists in the thermodynamically favoured chair conformation, and flip-flop interconversion between the chair- through boat-conformations are unlikely to occur. Moreover, internal motions are restricted [33], so that the pyranoside unit may be considered as a rigid entity. Small amplitude vibrational oscillations about the glycosidic bridges remain possible. Altogether, motions over a range of times shorter than overall tumbling of the molecule may potentially contribute to glycogen relaxation.

(1) We considered the dipolar spectral density function as a sum of lorentzians centred at zero frequency. Based on dynamic simulation and heteronuclear NMR studies of glucose pyranoside

units [33], we assumed that contribution from internal motions in the picosecond range could be neglected. The spectral density functions of all proton pairs of the pyranoside unit could then be adequately described by the same lorentzian i.e. monoexponential auto-correlation functions with the same single correlation time τ_i. Such an assumption leads to an analytical solution of eq (3) [15]:

$$\langle I_z \rangle = \frac{\cos\ \theta I_0}{\cos^2\theta + K\sin^2\theta} \tag{4}$$

with

$$K(\tau_i) = \frac{10 + 37\omega^2\tau_i^2 + 12\omega^4\tau_i^4}{10 + 16\omega^2\tau_i^2} \tag{5}$$

This model assumes that the dipolar interactions of *all* proton pairs are averaged by the motion of the pyranoside unit on a time scale of the order of τ_i, implying that its movements must be sufficiently free for each internuclear dipolar interaction vector to cover with equal probability all orientations $(\Omega = \theta, \varphi)$ relative to the B_0 direction on this time scale[3].

(2) Another way in which the dipolar interactions might average out, consists in the superposition of an internal motion of the pyranoside unit and of a slower movement, such as overall tumbling of the molecule. Recalling that the rotation time of the roughly spherical β particles can be estimated to be of the order of 1 to 10 μs, it seemed fair to separate these slow motions and those of the pyranoside rings into distinct terms. The dipolar spectral density function for each pair of spins α and β could then be written:

$$J_{\alpha\beta}(\omega) = \frac{1}{10}\frac{\gamma^4\hbar^2}{r_{\alpha\beta}^6}\left(\frac{S^2\tau_0}{1+\omega^2\tau_0^2} + \frac{(1-S^2)\tau_i}{1+\omega^2\tau_i^2}\right) \tag{6}$$

with a long correlation time $\tau_0 \sim 1/\Omega$ characteristic of the rotational diffusion process, a short correlation time $\tau_i \sim 1/\omega$ characteristic of rapid reorientation of the pyranoside units, and S^2 a generalised order parameter which characterises spatial restriction of motion. In this modified Lipari–Szabo type model [34], internuclear distances can reasonably be supposed constant in a local geometrical domain characterised by a single correlation time τ_i. The steady-state magnetisation of each spin $\langle I_z^\alpha \rangle$ is then equal to $\langle I_z \rangle$ and calculated from eq (3) [16]:

$$\langle I_z \rangle = \frac{\cos\theta I_0}{\cos^2\theta + \sin^2\theta\left(\frac{10+37\omega^2\tau_i^2+12\omega^4\tau_i^4}{10+16\omega^2\tau_i^2} + \frac{S^2}{1-S^2}\frac{\tau_0}{\tau_i}\frac{B}{A}\right)} \tag{7}$$

where,

$$A = \frac{1}{1+\omega^2\tau_i^2} + \frac{4}{1+4\omega^2\tau_i^2}$$

and

$$B = \frac{3}{2}\left(\frac{\cos^2\theta}{1+\Omega^2\tau_0^2} + \frac{\sin^2\theta}{1+4\Omega^2\tau_0^2}\right)$$

(3) So far, we have supposed τ_0 to be on the time-scale of the Debye rotation of the molecule. Other types of collective movements, as for instance motion of several pyranoside rings, might be expected to contribute to the averaging of the dipolar interactions to zero, as in amylose [31]. For these, we would expect the following constraints:

- their correlation times τ_L should be larger than τ_i (since a larger weight must be displaced),
- if they are larger than the overall dipolar correlation time τ_0, they cannot be detected.

A case which appears to be relevant to glycogen, is when there is sufficient freedom of internal motion, but when no contributions to relaxation resulting from motions in the microsecond range can be detected, i.e., $\tau_i << \tau_L << \tau_0$. Again, if we reason in terms of overall Debye correlation times, this implies that the dipolar interactions must vanish as a result of internal motions. For $\tau_i << \tau_L$, we can again assume a separation of motions. A way to describe this model is then to replace τ_0 by τ_L in eq (6) and to consider $1/\omega << \tau_L << 1/\Omega$. The analytical solution of the steady-state magnetisation

[3] This image is, rigorously speaking, too restrictive since motions other than isotropic can average out the dipolar interactions of a proton pair (e.g., [34]). However, as the steady-state magnetisation measured is an average value depending on *all* dipolar interactions, these must average out on the same time scale, whatever their direction in the pyranoside unit. Involvement of a jump model is unlikely in the case of a chain of pyranoside units, where intra- and inter-cyclic motions are restricted. We will nonetheless continue using this simplistic image, while keeping in mind these theoretical remarks for the subsequent interpretation of experimental results.

is then identical to eq (4) except that the constant K becomes:

$$K(S^2, \tau_L, \tau_i) = \frac{1}{10 + 16\omega^2\tau_i^2}\left(10\left(1 + \frac{3}{10}\frac{\tau_L}{\tau_i}\frac{S^2}{1-S^2}\right) + 37\omega^2\tau_i^2\left(1 + \frac{15}{37}\frac{\tau_L}{\tau_i}\frac{S^2}{1-S^2}\right) + 12\omega^4\tau_i^4\left(1 + \frac{\tau_L}{\tau_i}\frac{S^2}{1-S^2}\right)\right) \quad (8)$$

It is therefore impossible, when measuring the steady-state magnetisation as a function of the angle θ at a single static field, to distinguish between the model of a free motion of the pyranoside unit and the combination of a restricted one and a chain motion using just a variation of the angle θ at one static magnetic field. However, these two models might be distinguished through the use of different static magnetic fields ω.

Population distribution as a function of motion. The use of size-fractionated glycogen reduces dynamic heterogeneity resulting from a distribution of molecular sizes. It also allows independent investigation of molecular weight as a parameter, through comparison of fractions of widely different sized molecules. However, since glycogen is a large irregularly branched biopolymer, it is not unlikely that pyranoside rings may exhibit dissimilar dynamics, even though their proton resonance frequencies cannot be distinguished. This heterogeneity of dynamics within glycogen has in fact already been suggested [13,35]. The dynamics should then be represented by a *non correlated* sum of m populations, each with a dipolar spectral density function $J(\tau_0, \tau_{Lm}, \tau_{im})$ where the correlation times depend on the chosen motional model and on the molecular domain. The observed steady-state magnetisation is then the weighted sum of the steady-state magnetisation from each domain, described by eqs (4) or (7) according to the model of motion.

In our case, the precision of measurements does not justify using a continuous population distribution. Instead, we have used a model comprising only two populations, each relaxing according to either eqs (4) or (7), to fit all the data. In the absence of observable contributions from slow motions, the solution to eq (3) with such a model is:

$$\langle I_z \rangle = \cos\theta I_0\left(\frac{P}{\cos^2\theta + \sin^2\theta K_1} + \frac{1-P}{\cos^2\theta + \sin^2\theta K_2}\right) \quad (9)$$

where K_1 and K_2 correspond to the K functions of populations P and 1–P, respectively. K_1 and K_2 may be independently described either in terms of both collective and internal movements characterised by τ_{L1}, τ_{i1} and τ_{L2}, τ_{i2}, respectively, as in eq (8), or in terms of single local correlation times τ_{i1} and τ_{i2} for each population, in the case of one lorentzian spectral density function per pyranoside unit (eq (5)).

When slow motions were observed, the model was extended to take them into account for one of the two populations, according to model (2) described by eq (6).

$$\langle I_z \rangle = \cos\theta\, I_0\left(\frac{p}{\cos^2\theta + \sin^2\theta\left(\frac{10+37\omega^2\tau_{i1}^2+12\omega^4\tau_{i1}^4}{10+16\omega^2\tau_{i1}^2} + \frac{S^2}{1-S^2}\frac{\tau_0}{\tau_{il}}\frac{B}{A}\right)} + \frac{1-P}{\cos^2\theta + \sin^2\theta\frac{10+37\omega^2\tau_{i2}^2+12\omega^4\tau_{i2}^4}{10+16\omega^2\tau_{i2}^2}}\right) \quad (10)$$

where previous notations are used. We consider only one population with slow motion contributions, again to avoid parameters in excess, compared to precision of measurement.

3. Results and discussion

Detection of slow motions.—Fig. 3 shows the value of the magnetisation intensity as a function of the angle θ and of the rf-field amplitude ω_1 for glycogen fractions central to each distribution for (i) α- (a38), (ii) β- (b50) particulate rat glycogen and (iii) commercial oyster (oy47) glycogen, dissolved in ^2H_2O. The dispersion of points for oyster (*oy*) and rat (*b*) samples in all fractions tested ($n = 5$ and $n = 4$, respectively) were within experimental error. In particular, the measured intensities were not ordered according to rf-field strength. Rat (*a*) samples ($n = 4$), however, clearly displayed an increase of magnetisation intensity with rf field strength for given values of θ, as

predicted by the theory when slow motions are present [16]. Thus, independently of the type of motion and of any model, these results demonstrate some contribution of slow molecular motion on a time scale longer than 0.2 μs for the α-particulate rat liver glycogen, whereas no such contribution can be detected for either oyster or rat β-particulate glycogen. Moreover, independence of the magnetisation from the effective field Ω at constant angle θ implies that processes of fast chemical exchange do not contribute to relaxation of the oyster and β-particulate glycogen [17].

Under the experimental conditions described, visible variation of intensity would have been expected for dipolar correlation time values between 0.2 μs and 1 ms, whatever the type of slow motion. Since no such effect was observed for β particles of rat liver or commercial oyster glycogens, it follows that dipolar interactions vanish on a time scale smaller than typically 0.2 μs, i.e., on a time scale smaller than the overall correlation time predicted by the Debye expression ($\tau_0 > 1$ μs). The fact that this is not the case for (*a*) rat liver glycogen with similar molecular weight to that of (*b*) or

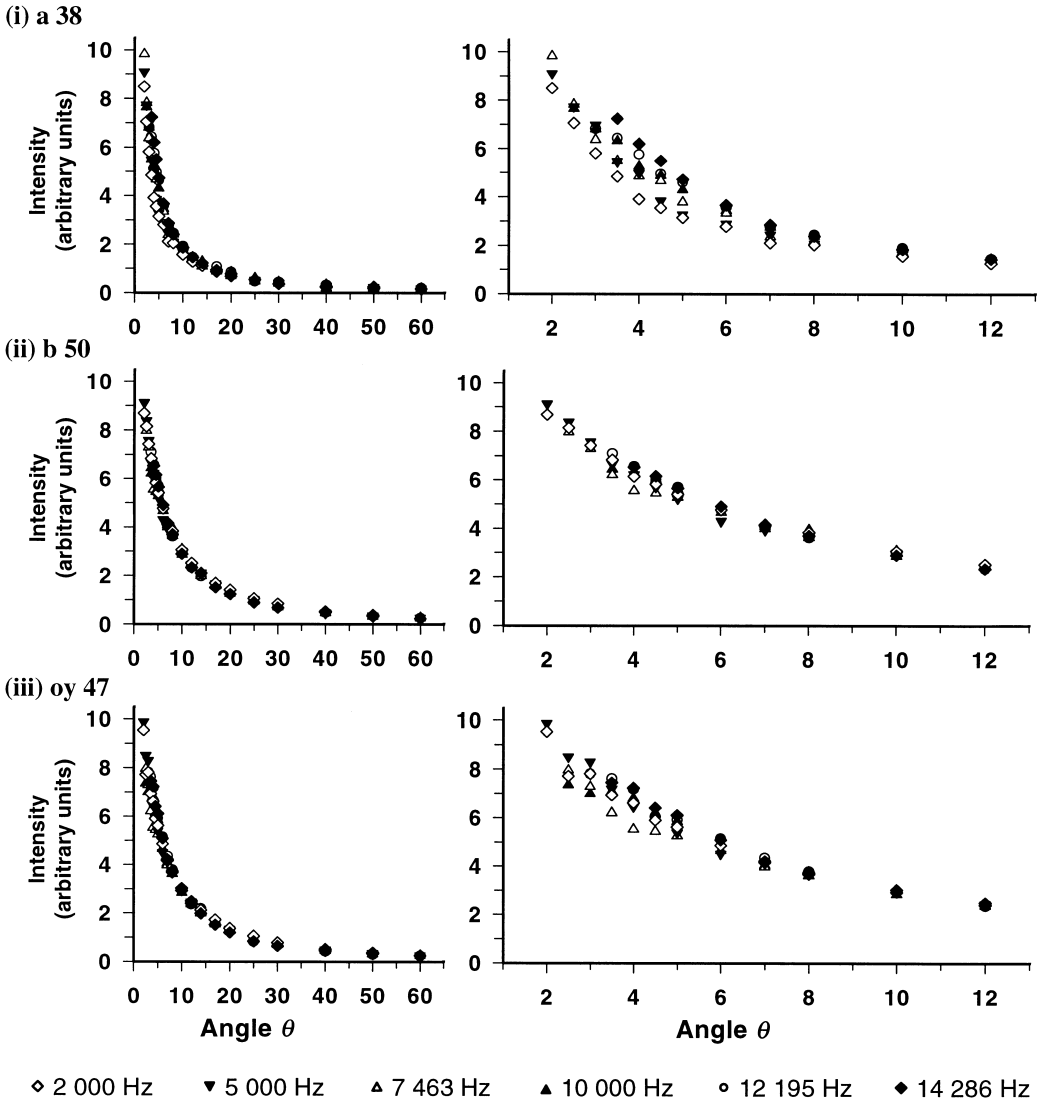

Fig. 3. Experimental signal intensities of steady-state magnetisation plotted against θ for six different rf field amplitudes ($\omega_1 = 14.3$, 12.2, 10.0, 7.5, 5.0 and 2.0 kHz) for central fractions of (i) (*a*), (ii) (*b*), and (iii) (*oy*) glycogen samples. The left hand-side plots show an expansion for θ between 2 and 12°, for which most variation is predicted. For β particles of rat liver (*b*) and oyster (*oy*) glycogen, the dispersion of intensities for a given θ remains within experimental error. For the α-particles of rat liver glycogen (*a*), the steady-state magnetisation intensities clearly depend on the effective field in a way compatible with contributions of motions to relaxation on a time-scale > 0.2 μs. Note, in particular the lowest and highest intensities for the smaller values of θ corresponding, respectively, to the weakest and strongest B_1 field amplitudes, which is not the case for the β particulate glycogens.

(*oy*) glycogen samples (e.g., a40 and oy40) is a clear indication of different internal structures inducing a variation of dynamics.

Measurement of steady-state magnetisation as a function of the angle θ.—Population models. Fig. 4 shows the measured intensity of the magnetisation as a function of angle θ for a fraction of β particles of rat liver glycogen, together with the best theoretical fit using eq (4) which disregards contributions from slow movement to relaxation (i). Clear departure of the curve is seen, as confirms the high value of reduced χ^2 ($\chi^2/v = 5.57$, $P = 4.75.10^{-44}$). The same was observed for all samples—including the oyster glycogen and the α particles—neither eq (4) nor eq (7) (for α particles) adequately described the dependence of the magnetisation on angle θ. This indicates that at least one of the assumptions underlying the theoretical expressions is wrong. These are pure dipolar relaxation, and either one lorentzian spectral density function per pyranoside unit or a combination of slower and faster internal motions. It seems difficult to invoke relaxation processes other than through dipolar interactions, fast chemical exchange or dissolved oxygen, which might contribute sufficiently to relaxation to provoke this distortion. No such deviation is present in other studies of oligosaccharides [14,15]. Rather, the distortion could result from a dispersion of motions within the glycogen molecule as already suggested in other studies [13,35]. The relative rigidity of the pyranoside units in the nanosecond range has been shown [33], justifying the assumptions leading to eq (7), at least in a local geometrical domain. These results have been corroborated by observations in larger oligosaccharides that dynamics of C–H pairs within the pyranoside ring were homogeneous but dynamics along the chain could vary [32]. In our particular case the use of fractionated glycogen proves that this distribution of motions resides within each glycogen particle and does not result from a distribution of molecular size. Consequently, the measured intensities were fitted against θ with the two-population model without slow motion contribution (eq (9)) for β particles of oyster and hepatic origin and with slow motion contributions (eq (10)) for the samples of α particles. The improved quality of the fits, illustrated in Fig. 4(ii), is obvious from the value of reduced χ^2. Here, $\chi^2/v = 0.171$, $P = 1.00$ with $F = 33.49$, $P = 6.01.10^{-33}$ compared by Snedecor test, to the single population fit.

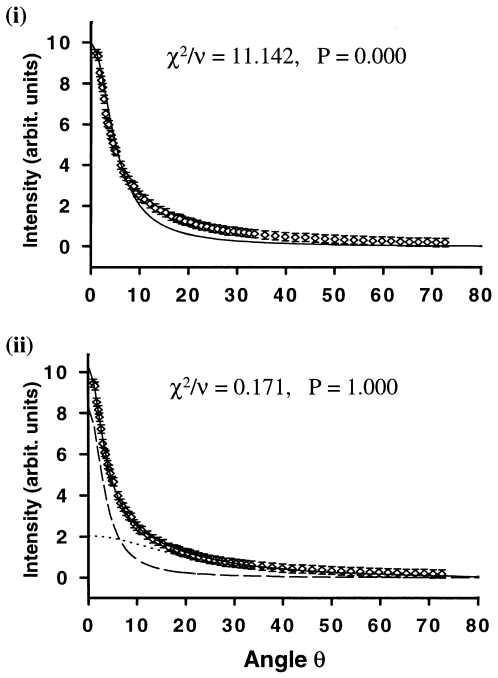

Fig. 4. Experimental signal intensities as a function of θ for fraction b47 from rat liver glycogen. Best-fits were calculated without slow motion contributions. A single population fit of b47 is shown in full curve (i). There is a clear deviation from the experimental data. A two-population fit of the same sample is represented in (ii) with the dashed f1(θ) and dotted f2(θ) lines showing the contribution from each population and in full line the total fit, in excellent agreement with experimental data.

Correlation time of the slow motions of α-particle glycogen. The data of α particles at six different B_1 fields displaying contributions from slow motion were fitted using eq (10). The results are presented for Fraction a38 for which the most values at very small angles ($\theta < 10°$) had been acquired. Fig. 5 shows the data and the best theoretical fits for each B_1 intensity on separate curves for clarity, even though these were calculated by a least squares fit of the six curves simultaneously, over the entire data set. The best fit was obtained for $\tau_{i1} = 9.7$ ns, $\tau_0 = 2.3$ μs, $\tau_{i2} = 1.9$ ns, $S^2 = 0.006$ and $P = 0.88$.

Regardless of the limited numerical precision of the model, two important points of information regarding slow motions may be gained from the fit of the data by a two-population model. The first concerns the order parameter S^2, which is defined as equal to 1 for a totally rigid molecule and to 0 for unrestricted motion. The calculated S^2 ranged from 0.006 to 0.018 for the different samples, always remaining much smaller than 1, indicating great internal mobility of the glycogen molecule on a time scale smaller than 1 μs. This result is in

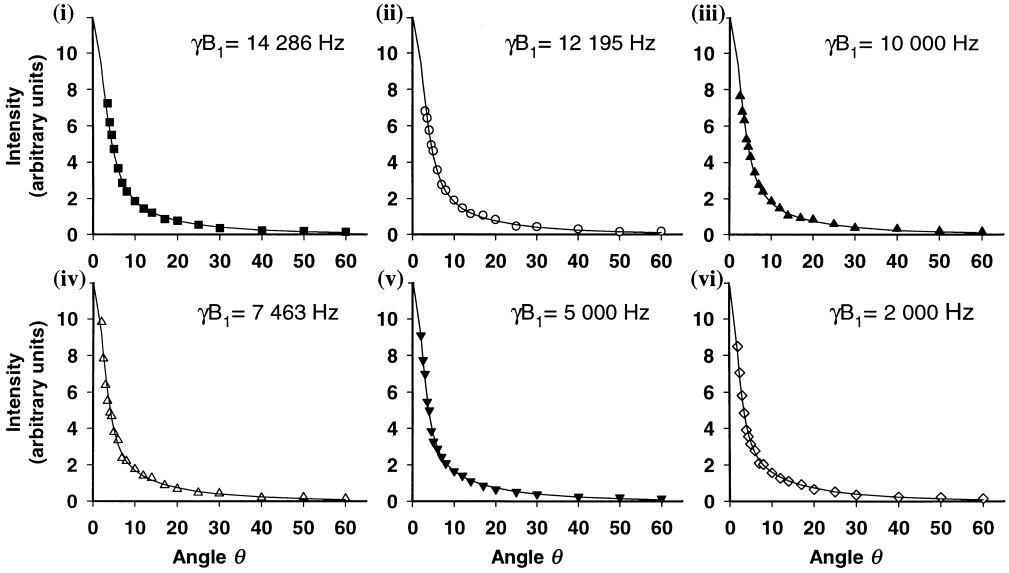

Fig. 5. Best fit of the two-population model including slow motion (eq (9)) to the experimental data of fraction a38 for the six rf field intensities shown on separate curves for clarity. (i) $\omega_1 = 14.3$ kHz, (ii) $\omega_1 = 12.2$ kHz, (iii) $\omega_1 = 10.0$ kHz, (iv) $\omega_1 = 7.5$ kHz, (v) $\omega_1 = 5.0$ kHz and (vi) $\omega_1 = 2.0$ kHz. Best fit parameters: $\tau_{i1} = 9.7$ ns, $\tau_0 = 2.3$ μs, $\tau_{i2} = 1.9$ ns, $S^2 = 0.006$ and $P = 0.88$.

relative agreement with the results for the other glycogen (*b*) and (*oy*) samples, for which no contribution ($S^2 = 0$ within experimental error) is observed. It agrees with previous NMR relaxation studies of glycogen, which find either little ($S^2 = 0.0022$ [11]) or no contribution ([2], $S^2 < 10^{-4}$ [13]) from the overall molecular motion and the fact that a small value of S^2 is required, in order to explain the NMR visibility of glycogen. The second point is that the correlation time for these slow motions, which we have estimated from our model to be 2.3 μs (ranging from 0.7 to 2.3 μs for other samples), is shorter by almost 2 orders of magnitude than the time of rotational diffusion which can be estimated from the Debye equation for a molecule the size of α-particulate glycogen (average diameter ~130 nm [22], $\tau_0 \sim 200$ μs), suggesting that the detected motions are more likely internal than overall. In fact they are closer to those expected for native β-particles (average diameter~40 nm, $\tau_0 \sim 5$ μs).

Comparison of the different glycogen samples.—To compare the different samples, measured intensities were fitted against θ with the two-population model which appeared to provide a better description of the dynamic behaviour. Fig. 6 compares best-fit parameters found for different glycogen samples. Both models with and without slow motions (eqs (10) and (9), respectively) systematically found that over 60% of spins relax with a longer correlation time, of the order of 10 ns, whereas the remaining spins $(1-P) < 0.4$ yielded a correlation time of the order of 1 ns. The functions governing the θ-dependence of the steady-state magnetisation of β-particles of rat and oyster glycogen, are indistinguishable in this model. None of the parameters P, τ_{i1} or τ_{i2} used for the fit differentiate the two types of sample. Rat liver α-glycogen however not only differs by the observable contribution of slow motion to relaxation—absent in oyster and β-particulate glycogen—but also by the higher proportion P, of slower relaxing spins. No overall correlation of the fit parameters could be found with size of the glycogen molecule.

Measurement at two B_0 *fields.*—To evaluate the quality of the model, the results were re-examined at a second static magnetic field. Since the numerical precision of our results is inevitably limited by the models used, we considered as a first approach that the systematic bias introduced by the processing of the spectra could be ignored for the sake of data comparison. This is acceptable as long as the processing is applied identically to all data. When comparing results at 7.05 and 11.7 Tesla, however, we feared that difference of separation (in Hz) between the glycogen and water resonances and in lineshape at the two fields, might influence the final results. Indeed, in our case, the main bias results from baseline corrections made necessary by the presence of the residual water resonance. We therefore first processed the data acquired at the two fields as described in Materials and methods.

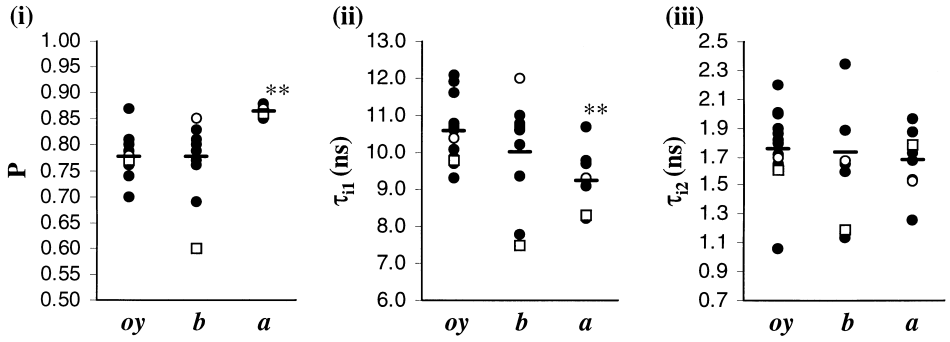

Fig. 6. Summary of the best-fit parameters of eq (9) for experimental points of (*b*) and (*oy*) glycogen samples and of eq (10) for (*a*) samples, for all fractions studied. In each category, the fractions central to the distribution are displayed (black circles) with the smallest (open square) and largest (open circle) molecular weights distinctly represented. For each glycogen type, the average value of the calculated parameter is shown (——). (i) proportion P, (ii) long correlation time (τ_{c1} from eq (8), τ_{i1} from eq (9)), (iii) short correlation time (τ_{c2} or τ_{i2}). A difference with better than 99% probability is observed (**) for the given parameters of (*a*) samples compared to (*oy*) and (*b*) samples.

We then re-analysed them after suppressing the water signal which was modelled in the time domain using parametric time analysis (HSVD). The resulting FID was processed in the time domain[4] by fitting a sum of damped sinusoids (VARPRO), (FIDAN© software from CRIS, Belgium). We also verified that integration of the H-1 (1→4) glycogen resonance after phase correction and a DC baseline correction of the Fourier transform of the water-suppressed data gave results within a few percent of those measured directly on the original spectra corrected for phase and baseline.

The results are shown in Table 1. As only one measurement was made at 11.7 T, the only statistically valid comparison is whether or not the fit at the higher B_0 field can be included in the group of measurements at lower B_0 field for which several measurements were made. In each category, we have excluded from the test the fractions with highest and lowest MW (cf. Materials and methods). For the (*oy*) sample, measurements did not differ at the two fields. For the (*b*) sample, the small differences observed depended on the processing of the data and must therefore be disregarded. These two results agree with those obtained for measurements at different B_1 fields: if there are contributions from slow motions to the relaxation of the β particles of either oyster or rat liver glycogen, they are within experimental error and are too small for us to detect. Moreover this result justifies a posteriori the use of a two population model to fit the data, rather than a distribution of populations. The precision on these results is unfortunately not sufficient to discriminate between the two models corresponding to the two expressions of K (eqs (5) and (8)). If eq (8) best described reality, a dependence of the measured τ_{i1} on B_0 field would be expected, but calculations with τ_L ranging from 10 ns to 1 μs and S^2 of up to 0.5 show at best a difference of 10% between the measurement of correlation times at 7.05 and 11.7 Tesla.

The α-glycogen fraction data were fit with eq (10) to take slow motions into account, fixing the S^2 value to 0.006 and the correlation time τ_0 for slow motion to 2.3 μs from measurements at different B_1 fields. In this sample, the longer internal correlation time τ_{i1} and the repartition of populations P were different at the two fields beyond 0.2% error, and the correlation time τ_{i2} of the smaller fraction differed with less than 2% chance of error, whatever the processing method. These results not only indicate that there is a definite B_0 field dependence of these types of samples as there was on B_1 field, confirming the influence of slow motions on the relaxation. They also show that the model we have used to take slow motions into

[4] Quantitating the glycogen resonance, whether in the time or frequency domains is equally problematic since the lineshape changes with θ (unpublished results). At small values of θ, the glycogen resonance invariably requires at least two linear exponentials for an adequate fit, as is usually observed for glycogen lineshape [36]. At large angles, however, only one exponential is needed. This correlates well with the two populations with shorter and longer relaxation times required for a satisfactory fit of dependence of the steady-state magnetisation on θ and the multiexponential T_2 decays observed by Overloop et al. [13]. We therefore fitted an excess number of lines to the residual FID, and considered those (one or two, depending on θ) found at the glycogen frequency.

Table 1
Best fit parameters obtained for three samples for which dependence of I_z on θ was measured at two B_0 fields, together with mean values of fits for sample of each type, measured at 7.05 T[a]

Sample type		Mean (7.05 T) ±SD	Sample	7.05 T		11.7 T	
				INTEG	VARPRO	INTEG	VARPRO
(*oy*)	τ_{il} (ns)	10.6 ± 0.9		10.1	10.6	11.5	9.9
	τ_{i2} (ns)	1.8 ± 0.3	**oy50**	1.7	2.0	2.0	2.5
	P	0.78 ± 0.04		0.78	0.74	0.81	0.73
(*b*)	τ_{il} (ns)	10.1 ± 1.1		9.4	7.8	8.6	7.7*
	τ_{i2} (ns)	1.7 ± 0.4	**b48**	1.6	1.2	1.3	1.2
	P	0.78 ± 0.05		0.76	0.83	0.87	0.87
(*a*)	τ_{il} (ns)	9.3 ± 0.9		8.2	10.7	6.1**	5.8**
	τ_{i2} (ns)	1.7 ± 0.2	**a35**	1.7	2.0	0.9**	0.5**
	P	0.87 ± 0.02		0.85	0.87	0.95***	0.95***

[a] The oyster and β-particulate glycogen data were fit with eq (11), τ_{i1} and τ_{i2} were calculated from eq (4). The α-particulate data was fit using eq (12), with $S^2 = 0.006$ and $\tau_0 = 2.3$ μs. Data was processed by integration in the frequency domain (INTEG) and linear exponential fitting in the time domain (VARPRO) as described in the text. Values significantly different from the mean of measurements at 7.05 T shown, for probabilities better than 10% error (*), better than 2% error (**) and better than 0.2% (***).

account is too simple to explain a most likely complex molecular motion. We do not however have the experimental precision to justify the use of a more complicated motional model which may describe the experimental results, i.e., we would no longer have the required precision to verify the assumptions.

4. Conclusions

For all the samples of fractionated glycogen that we studied, we observed that the dipolar interactions vanished on a time scale much shorter than the overall correlation time calculated from the Debye equation. The longest relevant dipolar correlation time was shorter than 0.2 μs for the β-particulate rat liver and oyster glycogens and of the order of the microsecond for α particulate rat liver glycogen. This result, which was independent of any model of motion, proves that internal dynamics of glycogen are sufficiently free to completely average out the dipolar interactions. The short time scale, and small contribution of these slow motions, also means the existence of a pool of pyranoside units with very restricted mobility is most unlikely. This pleads in favour of total visibility of the glycogen molecule to the NMR experiment, at least in vitro.

We were able to describe the dependence of the steady-state magnetisation as a function of the effective field angle θ through a simple model of dynamics based on the idea that various pyranoside units of the same glycogen molecule can undergo different uncorrelated motions. A model of two populations sufficed to fit our data. For all samples, two correlation times in the nanosecond time scale were obtained, one τ_{i1} of the order of 10 ns and the second one τ_{i2} of the order of 1 ns. These values were calculated by assuming a single local correlation time (eq (5)). They could instead, have been calculated from a model of combined slower and faster internal motion (eq (8)), i.e., with an internal motion, typically around 1 ns, and slower chain motions between 10 and a few hundreds nanoseconds, allowing exploration of the large area of orientations by the pyranoside units' directions. The precision of the measurements at two static magnetic fields is not sufficient to discriminate between these two models although the latter is the more likely for two reasons. Firstly, all pyranoside units should explore every orientation within 10 ns in order to average out dipolar interactions. Restricted motions of middle chain units makes this rather unlikely. Secondly, we were able to detect internal motions with correlation times of the order of the microsecond for α-particulate rat liver glycogen, corresponding to time scales of motion for intermediate structures.

The comparative measurement of the steady-state magnetisation as a function of the rf-field amplitude and of the effective angle θ has revealed a striking difference of the internal dynamics of α particles of rat hepatic glycogen relative to the β-particulate rat liver and oyster glycogens. This difference appears first in the dependence of the steady-state magnetisation on the rf-field amplitude at constant angle θ which can be detected only in α-particulate rat liver glycogen. This result is not

only due to the size of α particles. Indeed fractions of β particles, even of high molecular weight, do not exhibit this behaviour, while small α particles do. This result, which is totally independent of any motional model, clearly indicates that the difference of structures between α and β particulate glycogen induces a difference in mobility. The value of the slow motions correlation time found for α particles is of the order of that expected for the constitutive β entities, and may possibly result from motions of the latter. Secondly, the model of two populations of pyranoside units exhibiting different dynamics is sufficient to describe the results obtained for β-particulate rat liver and oyster glycogens, and gives consistent results if the dynamics are re-explored at an other static magnetic field. In contrast, for α-particulate rat liver glycogen, such a model is not adequate. It consequently appears that, certainly due to their constitutive structure, the description of internal dynamics of α particles requires a complex distribution of motions whose characteristic time scales range from less than 1 ns to more than 1 μs.

Acknowledgements

Professors M. Guéron and M. Goldman are greatly acknowledged for stimulating discussion.

References

[1] L.-H. Zang, D.L. Rothman and R.G. Shulman, *Proc. Natl. Acad. Sci. USA*, 87 (1990) 1678–1680.
[2] L.O. Sillerud and R.G. Shulman, *Biochemistry*, 22 (1983) 1087–1094.
[3] J.R. Brainard, J.Y. Huston, D.E. Hoekenga and R. Lenhoft, *Biochemistry*, 28 (1989) 9766–9722.
[4] B. Kunnecke and J. Seelig, *Biochim. Biophys. Acta*, 1095 (1991) 103–113.
[5] G. Bloch, private communication,
[6] P. Jehenson, D. Duboc, G. Bloch, M. Fardeau and A. Syrota, *Neuromuscul. Disord.*, 1 (1991) 99–101.
[7] D.L. Rothman, I. Magnusson, L.D. Katz, R.G. Shulman and G.I. Shulman, *Science*, 254 (1991) 573–576.
[8] I. Magnusson, D.L. Rothman, L.D. Katz, R.G. Shulman and G.I. Shulman, *J. Clin. Invest.*, 90 (1992) 1323–1327.
[9] P.C. Calder and R. Geddes, *Int. J. Biochem.*, 24 (1992) 71–77.
[10] A. Abragam, *Principles of Nuclear Magnetism*, Clarendon Press, Oxford (1961).
[11] L.-H. Zang, M.R. Laughlin, D.L. Rothman and R.G. Shulman, *Biochemistry*, 29 (1990) 6815–6820.
[12] W. Chen, X.-H. Zhu, M.J. Avison and R.G. Shulman, *Biochemistry*, 32 (1993) 9417–9422.
[13] K. Overloop, P. Van Hecke and F. Vanstapel, *Magn. Res. Med.*, 36 (1996) 45–51.
[14] M. Goldman and H. Desvaux, *C. R. Acad. Sci. Paris*, 317 (1993) 749–756.
[15] H. Desvaux and M. Goldman, *Mol. Phys.*, 81 (1994) 955–975.
[16] H. Desvaux, C. Wary, N. Birlirakis and P. Berthault, *Mol. Phys.*, 86 (1995) 1049–1058.
[17] H. Desvaux, N. Birlirakis, C. Wary and P. Berthault, *Mol. Phys.*, 86 (1995) 1059–1073.
[18] M. Borgs, P. Van Hecke, K. Overloop, C. Decanniere, S. Van Huffel, W. Stalmans and F. Vanstapel, *NMR Biomed.*, 6 (1993) 371–376.
[19] R. Laskov and E. Margoliash, *Bull. Res. Council Israel A*, 11 (1963) 351–362.
[20] G.T. Cori, *J. Biol. Chem.*, 96 (1932) 259–269.
[21] E. Bueding and S.A. Orrell, *J. Biol. Chem.*, 239 (1964) 4018–4020.
[22] P.C. Calder, *Int. J. Biochem.*, 23 (1991) 1335–1352.
[23] J.A. Reynolds, Y. Nozaki and C. Tanford, *Anal. Biochem.*, 130 (1983) 471–474.
[24] C.R. Krisman, *Anal. Biochem.*, 4 (1962) 17–23.
[25] P. Drochmans, *J. Ultrastruct. Res.*, 6 (1962) 141–163.
[26] R. Laskov and J. Gross, *Isr. J. Med. Sci.*, 1 (1965) 26–42.
[27] X. Yang, M.A. Miller, R. Yang, D.F. Evans and R.D. Edstrom, *FASEB J.*, 4 (1990) 3140–3143.
[28] R. Geddes, J.D. Harvey and P.R. Wills, *Biochem. J.*, 163 (1977) 201–209.
[29] W.H. Press, B.P. Flannery, S.A. Teukolsky and W.T. Vetterling, in *The Art of Scientific Progamming. Numerical Recipes in C*. Cambridge University Press, Cambridge, 1988.
[30] I. Solomon, *Phys. Rev.*, 99 (1955) 559–565.
[31] P. Dais, *Carbohydr. Res.*, 160 (1987) 73–93.
[32] L. Mäler, J. Lang, G. Widmalm and J. Kowalewski, *Magn. Res. Chem.*, 33 (1995) 541–548.
[33] P.J. Hajduk, D.A. Horita and L.E. Lerner, *J. Am. Chem. Soc*, 115 (1993) 9196–9201.
[34] G. Lipari and L. Szabo, *J. Am. Chem. Soc*, 104 (1982) 4546–4559.
[35] C.L. Jackson and R.G. Bryant, *Biochemistry*, 28 (1989) 5024–5028.
[36] K. Overloop, P. Van Hecke, F. Vanstapel, K. Overloop, H. Chen, S. Van Huffel, A. Knijn and D. Van Ormondt, *NMR Biomed.*, 9 (1996) 315–321.